
COMPARING METHODS TO ESTIMATE CLOUD COVER OVER THE BAIKAL NATURAL TERRITORY IN DECEMBER 2020

S.V. Podlesnyi 
*Institute of Solar-Terrestrial Physics SB RAS,
Irkutsk, Russia, step8907@mail.ru*

E.V. Devyatova 
*Institute of Solar-Terrestrial Physics SB RAS,
Irkutsk, Russia, devyatova@iszf.irk.ru*

A.V. Saunkin 
*Institute of Solar-Terrestrial Physics SB RAS
Irkutsk, Russia, saunkin@inbox.ru*

R.V. Vasilyev 
*Institute of Solar-Terrestrial Physics SB RAS,
Irkutsk, Russia, roman_vasilyev@iszf.irk.ru
Irkutsk State University, Irkutsk, Russia*

Abstract. The paper addresses the issue of how much cloud cover data obtained using satellite and model-interpolation techniques are suitable for monitoring the transparency of the atmosphere and determining conditions for airglow observations at a local geophysical observatory. For this purpose, we compared the temporal dynamics of cloud cover from ECMWF's ERA5 reanalysis and NOAA satellites with the night atmosphere transparency according to a digital camera. We considered the dynamics of the addressed parameters at the Geophysical Observatory of the Institute of Solar-Terrestrial Physics, located in the Baikal Natural Territory near Tory village (Republic of Buryatia, Russia), during December 2020. The comparative analysis

showed a generally good agreement between cloud cover data from ECMWF's ERA5 climate reanalysis and those observed with the camera. Disadvantages are the lack of information on rapid variations in cloud cover in the reanalysis and positive and negative delays in the dynamics of cloud fields that last about two hours. Due to irregular satellite data, large time gaps between passes, and difficulties in estimating cloud cover at night, we could not come to reliable conclusions concerning the applicability of satellite data.

Keywords: cloud cover; atmospheric transparency; ECMWF's ERA5 reanalysis; satellite observations

INTRODUCTION

In the south of Eastern Siberia, there are observatories of the Institute of Solar-Terrestrial Physics of the Siberian Branch of the Russian Academy of Sciences (ISTP SB RAS) equipped with instruments to investigate near-Earth space, near and deep space in the optical range. When passing through the atmosphere, optical radiation is subject to various distortions in the air inhomogeneities, which affects the quality of astronomical data (star image jitter, quality of diffraction pattern of star images, deformation of the solar edge image) and airglow observations. Important factors affecting the quality of optical observations are the moon phase and meteorological conditions. The main meteorological characteristic responsible for effectiveness of optical observations is the number of clear sky days or nights for a certain period (clear sky frequency [Darchia, 1985]) at the point of observations. It should also be noted that some local meteorological factors (e.g., frequency of fogs in the clear sky in a given area) can influence the observational conditions. Moreover, anthropogenic factors, such as direct and scattered light from different light sources, smog, haze, mist and dust, affect the quality of optical observations greatly. The influence of anthropogenic factors can be eliminated by taking the observation point to a sufficient distance from settlements and industrial zones. The effect of the atmospheric column processes can be taken into account only after preliminary long-term observations of weather conditions at an expected observation point. For instance, the monograph by Sh.P. Darchia

[1985] deals with studying the frequency of clear sky and other astroclimatic characteristics in the USSR. The author substantiated the choice of southern regions of Eastern Siberia to build optical observatories of ISTP SB RAS (SibIZMIR at that time).

Large-scale circulation and weather conditions change over time. We are interested in monitoring the atmospheric transparency and studying the climatic variability of basic meteorological parameters directly related to the concept of clear sky frequency and atmospheric transparency at the ISTP SB RAS optical observatories. It is essential for diagnosing the main regularities in the variability of airglow observation conditions and for assessing their possible future changes. The main parameter that is directly related to the concept of clear sky frequency and largely determines optical observation conditions is cloud cover.

Selecting data for research is a major challenge. This problem is perfectly solved on a global scale by reanalysis projects providing information on different meteorological parameters at different atmospheric heights at regular latitude-longitude grid points with different time resolutions over several decades. For instance, Shikhovtsev et al. [2020] present the results of using NCEP/NCAR Reanalysis, ECMWF ERA-40, and ERA-Interim data for analyzing meteorological and optical characteristics of the atmosphere at ISTP SB RAS Sayan Solar Observatory (SSO). In our study, we use the ERA5 project [Hersbach et al., 2020] of the European Centre for Medium-Range Weather Forecasts (ECMWF) [<https://www.ecmwf.int/>]. ERA5 is the fifth

generation ECMWF reanalysis for the global climate and weather for the past 4 to 7 decades. As in other reanalyses, in ERA5 large-scale cloud cover is a calculated characteristic. The large-scale cloud and precipitation scheme in this project is based on the scheme proposed by Tiedtke [1993]. This scheme was then upgraded with improved representation of mixed-phase clouds [Forbes, Ahlgrimm, 2014], and prognostic variables for precipitating rain and snow [Forbes, Tompkins, 2011; Forbes et al., 2011]. In addition, there were numerous improvements to the parametrization of microphysics [Ahlgrimm, Forbes, 2014]. Improvements were also made to the scheme of convection parameterization originally proposed in [Tiedtke, 1989], and in a number of other schemes related to cloud cover representation.

Another option to obtain data on cloud cover is satellite observations. At present, more than a dozen global cloud databases based on satellite observations exist and are extensively used. Also, to date a number of works comparing satellite data on cloud cover with data from ground-based observations and reanalysis projects have been published. For example, Qinglong You et al. [2014] compare cloud cover from NCEP/NCAR and ERA-40 reanalyses with ground-based observations for the Tibetan Plateau. Lei et al. [2020] present the results of comparing cloud cover from satellite observations with that from ERA5 and ERA-Interim projects over the Tibetan Plateau and Eastern China.

To assess the reliability of reanalysis and satellite data for the local observatory of interest, we should compare them with ground-based observations. Unfortunately, there are no regular meteorological observations for the ISTP SB RAS observatory; therefore, we can compare only indirect data. In this paper, we compare data on total cloud cover from the National Oceanic and Atmospheric Administration (NOAA) satellites and ECMWF's ERA5 reanalysis with data on the night atmosphere transparency from the wide-angle digital camera FILIN-1C installed at the Geophysical Observatory of ISTP SB RAS, Tory village, the Republic of Buryatia, Russia. Note that the camera is not designed specially to monitor cloud cover, but can be successfully adopted for this purpose. The technique for estimating atmospheric transparency and cloud cover with the aid of the digital camera FILIN-1C is described below. We are not pioneers in using digital camera observations for estimating cloud cover. In [Zagainova, Karavayev, 2013], one can learn about a method for automatic determination of cloud amount from images taken in the visible range by the all-sky camera installed at ISTP SB RAS SSO.

The purpose of this work is to find out how much ECMWF's ERA5 and satellite data are suitable to monitor the transparency of the winter night atmosphere and the cloud cover at a particular ground-based optical observatory (Geophysical Observatory of ISTP SB RAS, Russia).

INSTRUMENTS AND DATA

Figure 1 shows mutual arrangement of the Geophysical Observatory, four ERA5 grid points, and the regions

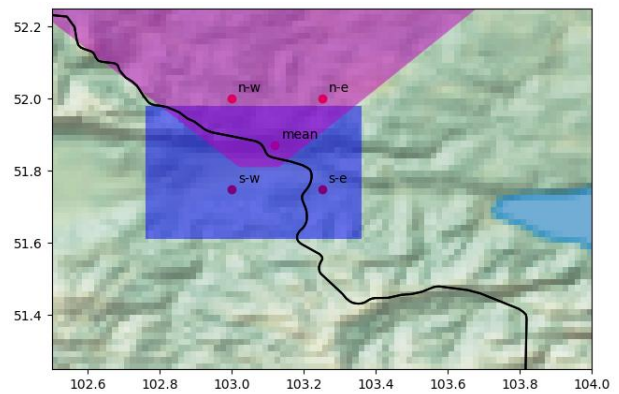


Figure 1. Location map of four ERA5 grid points nearest to the Geophysical Observatory and 'mean' point (red dots), area of satellite data collection (blue region), and FILIN-1C camera viewing angle (magenta)

where cloud cover was observed from satellite and FILIN-1C data. Red dots with coordinates s-w (51.75 N, 103.00 E), n-w (52.00 N, 103.00 E), s-e (51.75 N, 103.25 E), and n-e (52.00 N, 103.25 E) correspond to ERA5 grid points. Satellite images are bounded by the region with coordinates 51.37 N – 51.59 N and 102.46 E – 103.22 E (blue region). Camera FILIN-1C is located at (51.81 N, 103.07 E), its angle is shown in green. For the study, we took the mean cloud cover value between ERA5 grid points, which corresponds to coordinates of the 'mean' point in Figure 1 (51.87 N, 103.12 E).

FILIN-1C wide-angle camera

CCD sensor-based devices are often used to assess atmospheric transparency and cloud cover. For example, in [Zdor, 2011; Kazakovtsev, Kolin'ko, 2019; Kokarev et al., 2019], cloud-free and cloud-cover regions of the sky are distinguished based on star density in CCD sensor images.

The FILIN-1C wide-angle camera is designed to detect airglow and its spatial and temporal variations, study natural and man-made space objects (meteors, spacecraft), monitor atmospheric transparency, and solve some other problems. As a recording device, the instrument employs a CCD camera VideoScan-11002/O/Π/2001 based on CCD matrix KODAK KAI-11002. Main parameters of the CCD camera: 4008×2672 pixel image resolution, 9×9 micron pixel size. To ensure that the light load of all matrix pixels exceeds the noise level, we set the exposure time to 300 s [Mikhalev et al., 2016].

To estimate atmospheric transparency, we use the number of stars in the camera field of view (FOV). Star images are characterized by brightness with strong spatial gradients, which are much higher than those for the background airglow. This, in turn, makes it possible to count the stars visible in the image, and identify them as image areas whose intensity is higher in relation to the background. When the atmospheric transparency changes due to clouds, mist or fog, the star brightness drops, intensity gradients weaken, and stars begin to blend into the background. Thus, it is possible to develop an algorithm for processing night-sky images. The algorithm will distinguish relevant groups of pixels (regions) ac-

ording to certain threshold brightness; the number of these groups to a certain accuracy will be equal to the number of stars in the camera FOV.

To perform the described image processing, we should first eliminate noise, vignetting effects, and increase the contrast. In this case, noise refers to hot pixels, which can be eliminated using a median filter with a 3×3 pixel rectangular core. The image intensity is then equalized by multiplying the intensity of each pixel by a relevant coefficient to reduce vignetting effects of the wide-angle lens. We use calibration images of uniform brightness to determine a set of these coefficients. Next, we increase image contrast and determine the threshold using which the resulting image is converted into binary form for further splitting into regions. These regions include both stars and other objects that have considerable intensity gradients and have been prefiltered using the above procedures. Areas that are not stars are eliminated using threshold selection by the size of the area. The algorithm of area and size identification and selection has been implemented using the library `scipy.ndimage.measurements`. label [arXiv:1907.10121 [CS.ms]]. On average, about four thousand stars can be seen in the FILIN-1C image of the moonless clear sky. A decrease in the total number of visible stars indicates decreased atmospheric transparency. The cloud criterion (K_c) is essentially the extent to which the camera FOV is shielded coverage by clouds. We calculated it by the formula:

$$K_c = (\max N_s - N_s) / \max N_s \cdot 100 \%$$

where N_s is the number of stars in the current frame, and $\max N_s$ is the maximum number of stars per frame during the entire time of observations considered.

ECMWF's ERA5 reanalysis

From ECMWF's ERA5 reanalysis [Hersbach et al., 2020] we took data on Total Cloud Cover (TCC). This parameter represents a cloud fraction of the grid box. TCC is a single level field calculated from cloud cover, which occurs at different model levels through the atmosphere, taking into account the assumptions about the degree of overlap/randomness between clouds at different heights. Cloud fractions vary from 0 to 1.

Data is presented at one-hour resolution on $0.25^\circ \times 0.25^\circ$ horizontal grid from 1979 to date. In this article, we use December 2020 data at four grid points nearest to the ISTP SB RAS Geophysical Observatory (Figure 1).

Satellite data

In this study, we use NOAA 18 and NOAA 19 images to estimate cloud cover. An algorithm for estimating cloud cover from multispectral brightness measurements made by the Advanced Very High Resolution Radiometer (AVHRR) on board NOAA polar-orbiting satellites is described in [Stowe et al., 1999]. In our work, we apply this algorithm. Images of the Earth surface to assess cloud cover were obtained using a hardware and software system Alice-SCTM designed for receiving and processing data transmitted from polar-orbiting artificial Earth satellites at 1.7 GHz. The Alice-

SCTM system has been developed and is maintained by SCANEX Holding [<https://www.scanex.ru/>]. Figure 2 shows an example of Alice-SCTM images with a cloud mask for the region under study. The cloud cover percentage is defined as the ratio of pixels occupied with cloud cover to the total number of mask pixels. The obtained time series of cloud cover dynamics contains rare and nonequidistant values since we employ data from polar-orbiting satellites that pass over the region of interest at irregular intervals.

RESULTS AND DISCUSSION

Figure 3 plots K_c according to FILIN-1C camera (blue), and cloud cover according to NOAA satellites (red dots) and ERA5 (green) in December 2020. December is divided into 10-day intervals for ease of analysis.

Figure 3 shows advantages and disadvantages of each of the three datasets, namely:

1. FILIN-1C data has good time resolution (5 min), but only for dark hours;
2. ERA5 data is continuous with 1 hr discreteness;
3. NOAA satellite data is irregular over time.

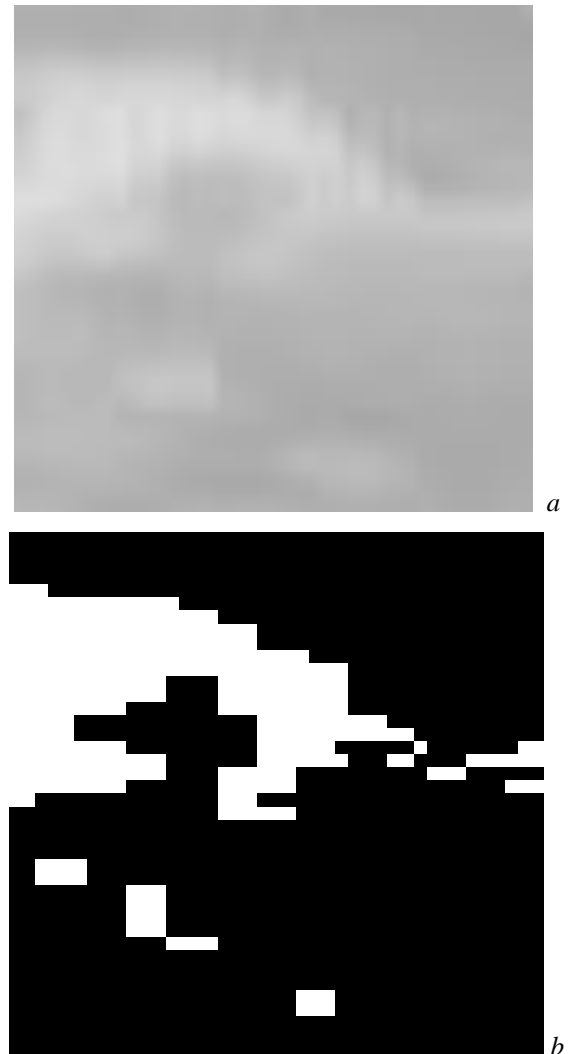


Figure 2. Cloud mask image for the region under study, taken by Alice-SCTM (a) and after processing (b).

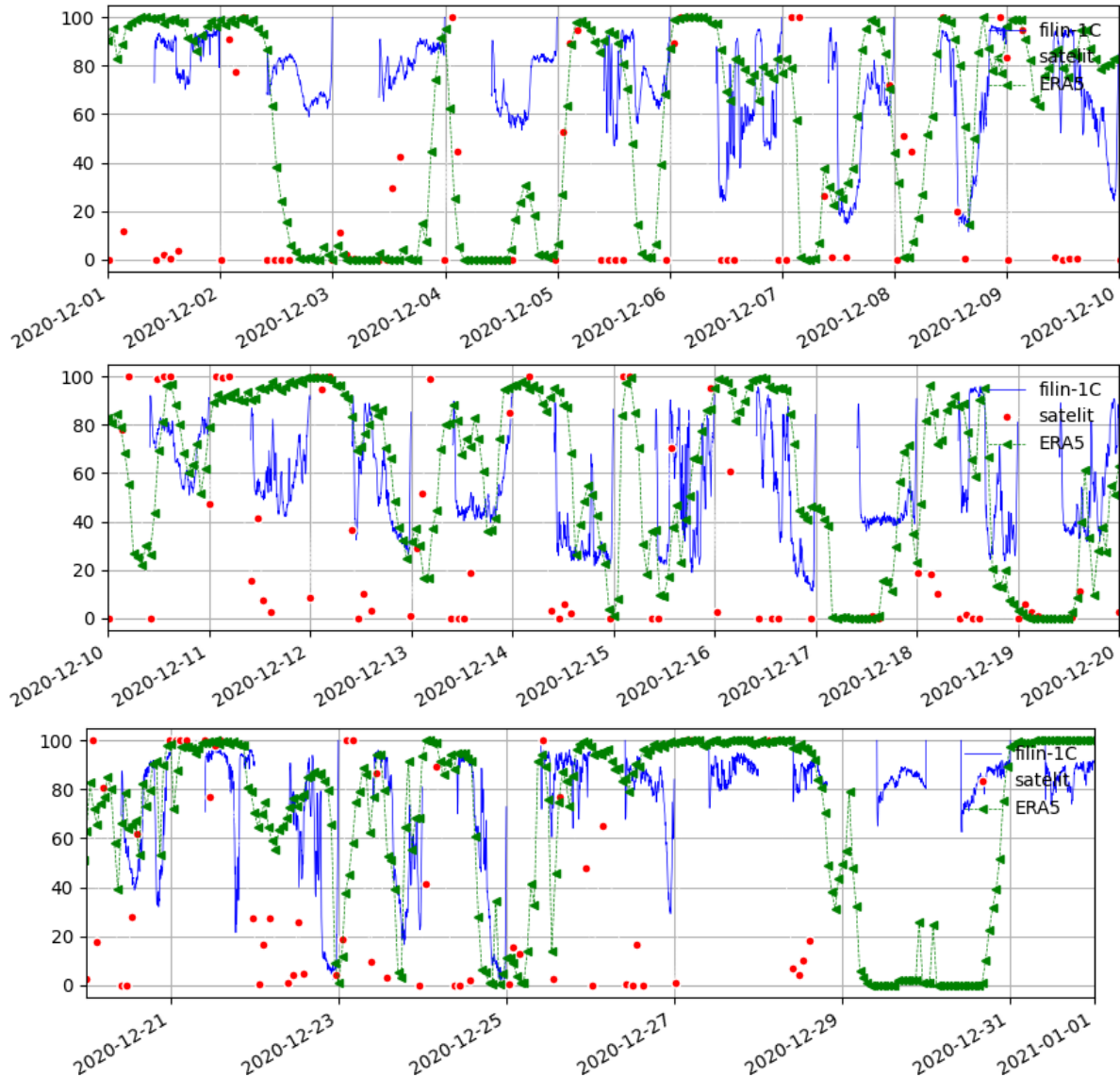


Figure 3. K_c (blue), cloud cover from satellites (red dots), and ERA5 total cloud cover (green). December 1–9, 2020 (a), December 10–19, 2020 (b), December 20–31, 2020 (c)

Figure 3 illustrates the main features of the inter-dynamics of the three datasets:

1. Time shifts between ERA5 and FILIN-1C data at different nights: December 07, 2020, December 08, 2020, December 10, 2020, December 14, 2020, December 22, 2020, December 23, 2020, and December 24, 2020. In Figure 4 are plots for December 08, 2020 and December 23, 2020 as examples.

2. Poor representation in ERA5 data of relatively rapid changes in cloud cover, which are clearly seen in FILIN-1C data. In Figure 5 are plots for the December 21, 2020 night demonstrating this feature: at ~19.00 UTC, FILIN-1C data has a pronounced K_c minimum that is not found in ERA5. Thorough analysis of the camera original images has revealed that this feature is due to short-term clearings (duration of several frames) within the camera coverage.

3. Low match between the cloud cover from satellites and that from ERA5 and FILIN-1C, especially at night. This is presumably due to the difficulty in estimating cloud cover from satellite data at night in winter.

In general, two parameters are used to determine a cloud mask – albedo and temperature difference. Unfortunately, in the algorithm for obtaining a cloud mask we employ, it is impossible to use the albedo parameter due to the lack of sun illumination. Moreover, the difference in temperatures between cloud cover and underlying surface varies over time. These conditions reduce the performance of the algorithm and lead to the need for coefficients to improve the cloud mask selection quality. Figure 6 shows plots for the December 16, 2020 and December 24, 2020 nights as an example of differences between data from satellites and from FILIN-1C and ERA5. For these two nights, we tried to change cloud mask selection settings (two bottom panels in Figure 6). The plots demonstrate improved quality of cloud selection during overcast, where it has not been previously detected. At the same time, the mask-selected percentage of cloud cover also increases during periods with low or zero cloud counts according to ERA5 and FILIN-1C, which leads to overestimated parameters (right-most points (after 22:00)).

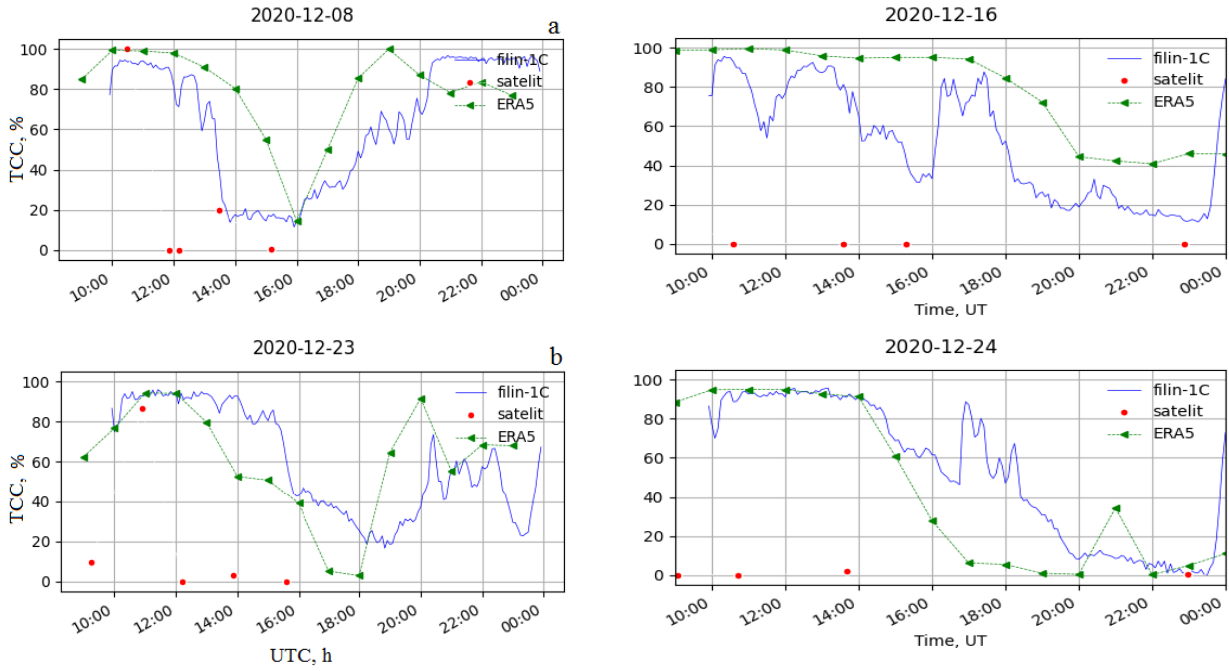


Figure 4. Plots of K_c (blue), cloud cover from satellites (red dots), and ERA5 total cloud cover (green) for December 08, 2020 (a) and December 23, 2020 (b) show time shifts between ERA5 and FILIN-1C data

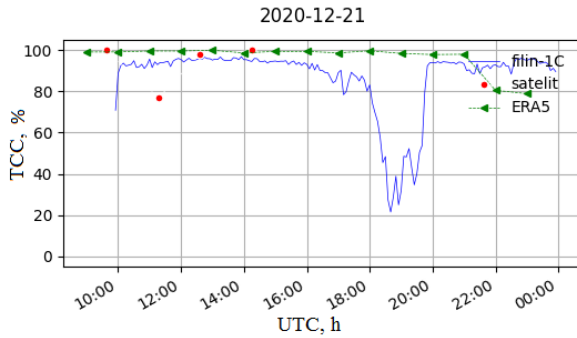


Figure 5. Plots of K_c (blue), cloud cover from satellites (red dots), and ERA5 total cloud cover (green) for December 21, 2020 illustrate poor representation of rapid changes in cloud cover in ERA5 data

This means that it is not quite correct to apply the same parameters of cloud mask selection to different lighting conditions (day and night hours). Apparently, to estimate cloud cover we should use the coefficients whose values will change during a day. Further, the values of coefficients and their variations can be determined using the described method of joint ground-based and satellite observations of cloud cover.

4. Early and late this month, there were a few nights that provoked our interest: there was an obvious discrepancy between K_c and ERA5 data, namely, K_c values were too high at low cloud values (December 02, 03, 04, 05, 29, and 30). Figure 7 presents plots for December 02, 2020 and December 29, 2020 demonstrating this feature. Thin clouds and the shine of the Moon proved to be a cause of the data discrepancy. The full-moon light during those nights was scattered by crystals of high thin clouds, or by the ice covering the camera protecting glass,

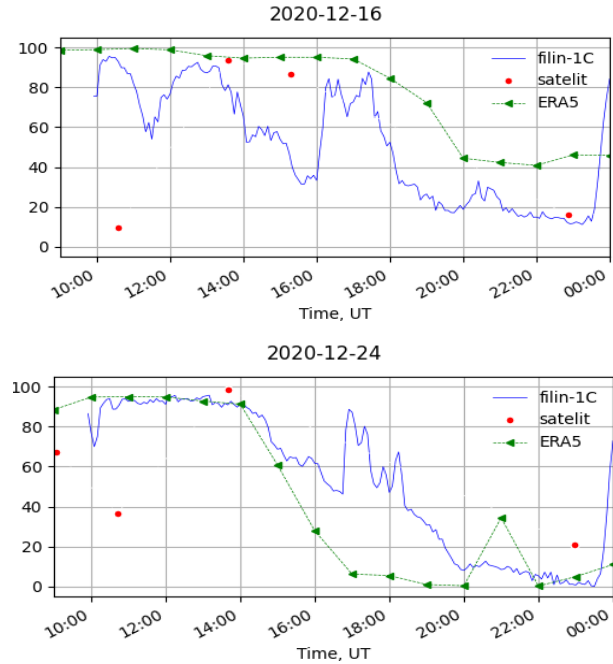


Figure 6. Plots of K_c (blue), cloud cover from satellites (red dots), and ERA5 total cloud cover (green) for December 16, 2020 and December 24, 2020, illustrating low match between cloud cover from satellites and from ERA5 and FILIN-1C (top panels) and improvement in the match after changing cloud-mask parameters (bottom panels)

and led to the data distortion. Thus, during the full-moon nights when the K_c criterion is used to identify cloud cover, we should bear in mind the risk of inaccurate representation of the real picture.

Six nights (December 09, 11, 13, 14, 19, and 26) required clarification of whether the cloud cover was high, medium or low. At these nights, relatively low K_c values correspond to relatively high values of cloud cover (i.e. the number of visible stars is great). Figure 8 shows plots illustrating this feature for the December 11 and 14, 2020 nights. Analysis of FILIN-1C original images

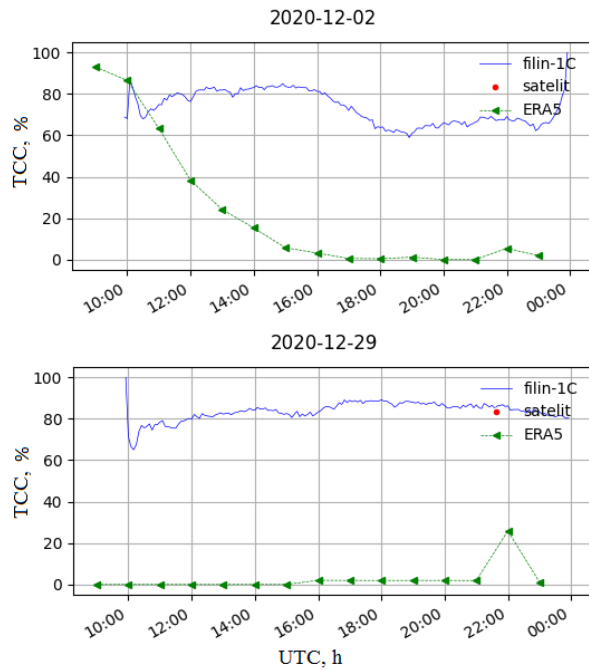


Figure 7. Plots of K_c (blue), cloud cover from satellites (red dots), and ERA5 total cloud cover (green) for December 02, 2020 and December 29, 2020, illustrating how the full-moon light scattered by thin cloud crystals affected FILIN-1C data

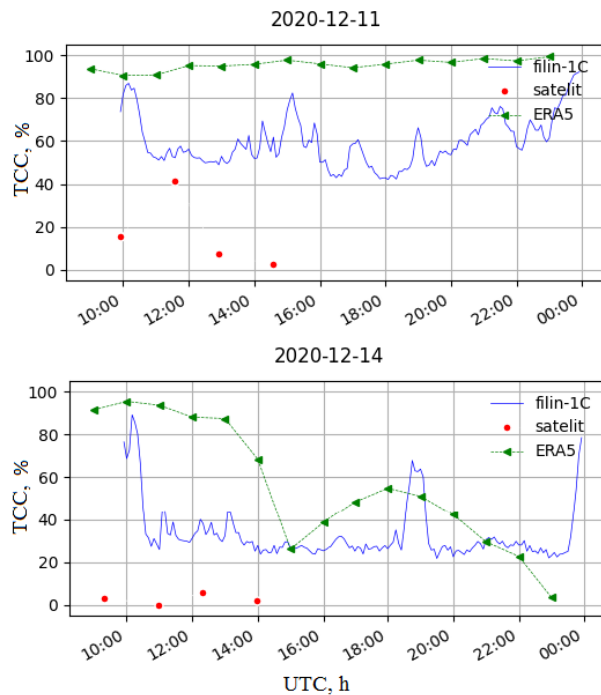


Figure 8. Plots of K_c (blue), cloud cover from satellites (red dots), and ERA5 total cloud cover (green) for December 11, 2020 and December 14, 2020, illustrating how thin cloud veil affected FILIN-1C data.

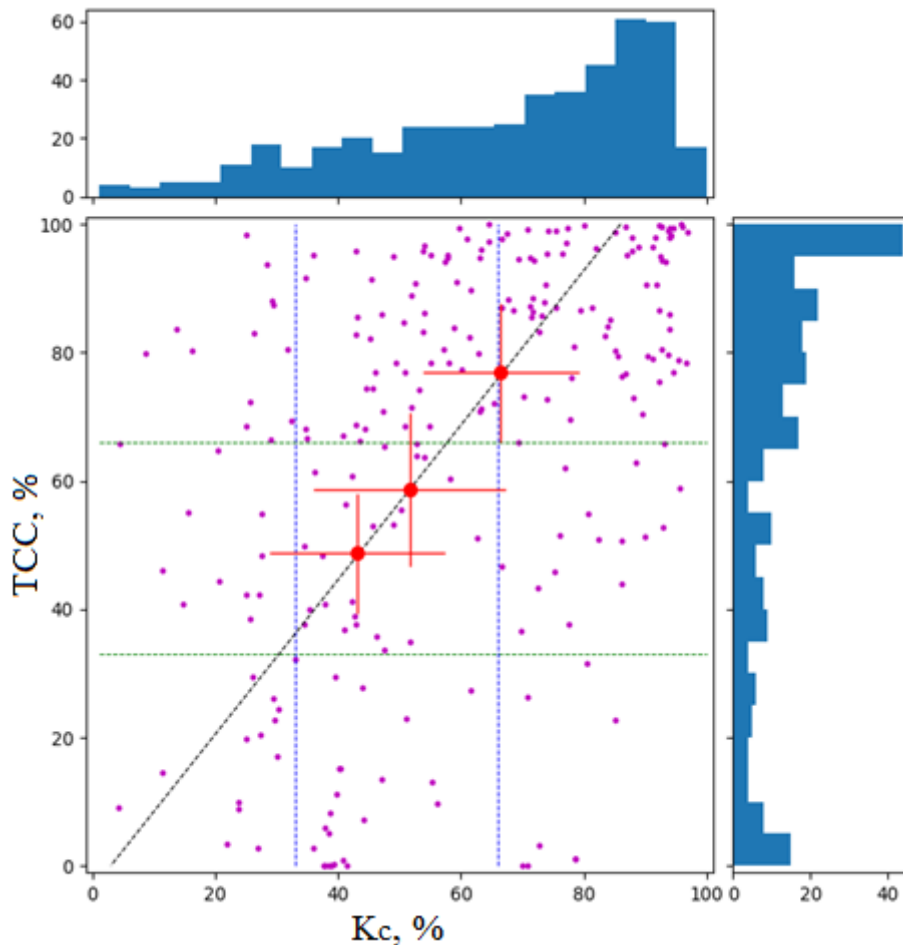
has revealed that at these nights an optically thin veil of cloud cover quite transparent for stars was observed. This influenced the results of calculating the K_c criterion. Bursts in K_c are caused by short-term concentrations of cloud cover in the camera FOV.

Figure 9 shows a diagram of K_c scatter and ERA5 cloud cover from which day and full-moon night data were removed. The strong variance of the diagram points is most likely to be associated with the nonstationary time lag between data from different sources (cameras and reanalysis) and rapid cloud cover variations detected by the camera and not displayed on reanalysis maps. Since it is impossible to determine whether the statistical distributions of the parameters considered are normal (small statistics and a certain asymmetry of distributions), it is not quite correct to calculate the standard correlation coefficient or apply minimizing methods to these datasets. There is a high probability of parameter bias due to the input data variance. To reduce the input data variance and to further assess the relation between the considered parameters, we have divided the initial distributions into three equal parts (0–33 %, 33–67 %, 67–100 %). In these parts, for each dataset we estimated the mean cloud cover and correlation parameter. For example, for 0–33 % cloud cover for ERA-5 (from the axis origin to the bottom green dotted line), the average cloud cover calculated from FILIN-1C is about 43 %. For the same range for FILIN-1C (from the axis origin to the left blue dotted line), the average cloud cover calculated from ERA-5 is about 42 % (see Figure 9). Thus, in the scatter diagram the resulting six averaged values form three points reflecting the desired relation. This data representation is more illustrative and allows us to see the linear relation between K_c and ERA5 cloud cover in a statistically poor dataset.

CONCLUSION

We have reviewed three datasets on cloud cover: from NOAA satellites, ECMWF’s ERA5 reanalysis, and FILIN-1C wide-angle camera, installed at the ISTP SB RAS Geophysical Observatory (Republic of Buryatia, Russia). When analyzing the results, technical features of all three datasets should be taken into account. For example, satellite systems have low sampling frequency and instability of measurements over time, which leads to large data gaps. Also, there are difficulties in estimating cloud cover from satellite data at night in winter. The reanalysis data is the product of the total cloud cover calculations on a stable spatial grid when clouds occur at different levels in the model atmosphere, given the assumptions about the degree of cloud overlap at different heights. The data cannot be attributed to observational data and needs to be validated for a selected region at a given time interval. Camera FILIN-1C data has good time resolution, but only for dark hours. In the presence of thin cloud scattering crystals during full-moon phases, the moonlight shine can negatively contribute to the images obtained with the camera.

Comparison of cloud cover data from satellite systems (NOAA) and the ECMW’s ERA5 reanalysis with K_c calculated from FILIN-1C images has revealed both match and difference in the data. From the material studied we can confidently say that during the nights without interference (moonlight scattered by thin cloud

Figure 9. K_c /ERA5 TCC diagram

crystals), ERA5 and FILIN-1C data are close agreement with each other. This gives us grounds to trust total cloud data from this reanalysis for optical and climatic studies in the Baikal Natural Territory. Nonetheless, the sampling frequency of the data over time is not quite sufficient to monitor observational conditions at the local optical observatory, because they do not represent rapid variations in the total cloud cover. Besides, we should remember that in the case of thin stratus clouds the obtained values of the K_c criterion (overestimated number of stars) can be lower compared to denser clouds. At the same time, the overall cloud dynamics from ERA5 and K_c is well correlated. Presumably, ERA5 slightly overestimates the cloud cover density compared to in-situ data. Yet, insufficient data for analysis does not allow us to make reliable judgements about it.

Due to irregularity in satellite data, large time gaps between flights, and the difficulty in estimating cloud cover for different lighting conditions (day and night) in winter, we could not draw reliable conclusions about applicability of satellite data. Apparently, to estimate cloud cover under different lighting conditions, we should use the cloud mask selection parameters that change during the day. Further, the coefficients and their variations can be determined using the described

method of joint ground-based and satellite observations of cloud cover.

The work was supported by the Ministry of Science and Higher Education of the Russian Federation (Grant No. 075-15-2020-787) for implementation of Major scientific projects on priority areas of scientific and technological development (the project «Fundamentals, methods, and technologies for digital monitoring and forecasting of the environmental situation on the Baikal natural territory»). The work was performed using data from Shared Equipment Center “Angara” [<http://ckp-rf.ru/ckp/3056>], ECMWF ERA5, NOAA.

REFERENCES

- Ahlgrimm M., Forbes R. Improving the representation of low clouds and drizzle in the ECMWF model based on ARM observations from the Azores. *Monthly Weather Review*. 2014, vol. 142, iss. 2, pp. 668–685. DOI: [10.1175/MWR-D-13-00153.1](https://doi.org/10.1175/MWR-D-13-00153.1).
- Darchia Sh.P. *Ob astronomicheskom climate SSSR* [On the astronomical climate of the USSR]. Moscow, Nauka Publ., 1985, 175 p. (In Russian).
- Forbes R.M., Ahlgrimm M. On the representation of high-latitude boundary-layer mixed-phase cloud in the ECMWF global model. *Monthly Weather Review*. 2014, vol. 142, iss. 9, pp. 3425–3445. DOI: [10.1175/MWR-D-13-00325.1](https://doi.org/10.1175/MWR-D-13-00325.1).
- Forbes R.M., Tompkins A.M. An improved representation of cloud and precipitation. *ECMWF Newsletter*. 2011, vol. 129,

pp. 13–18. DOI: [10.21957/nfgulzhe](https://doi.org/10.21957/nfgulzhe).

Forbes R.M., Tompkins A.M., Untch A. A new prognostic bulk microphysics scheme for the IFS. *ECMWF Technical Memorandum No. 649*. 2011, 28 p. DOI: [10.21957/bf6vjvxx](https://doi.org/10.21957/bf6vjvxx).

Hersbach H., Bell B., Berrisford P., Hirahara S., Horányi A., Muñoz-Sabater J., Nicolas J., Peubey C., Radu R., Schepers D., et al. The ERA5 Global Reanalysis. *QJRM*. 2020, vol. 146, iss. 730, pp. 1999–2049. DOI: [10.1002/qj.3803](https://doi.org/10.1002/qj.3803).

Kazakovtsev A.F., Kolin'ko V.I. Method for estimating cloudiness of night atmosphere and a night cloud sensor for implementation thereof. Patent RU 2678950 C1. 2019.

Kokarev D.V., Galileiskii V.P., Morozov A.M., Elizarov A.I. Device for observing the optical state of the sky within the visible hemisphere. Patent RU 191582 U1. 2019.

Lei Y., Letu H., Shang H., Shi J. Cloud cover over the Tibetan Plateau and eastern China: a comparison of ERA5 and ERA-Interim with satellite observations. *Climate Dynamics*. 2020, vol. 54, pp. 2941–2957. DOI: [10.1007/s00382-020-05149-x](https://doi.org/10.1007/s00382-020-05149-x).

Mikhalev A.V., Podlesnyi S.V., Stoeva P.V. Night airglow in RGB mode. *Solar-Terrestrial Physics*. 2016, vol. 2, iss. 3, pp. 106–114. DOI: [10.12737/22289](https://doi.org/10.12737/22289).

Qinglong You, Yang Jiao, Houbo Lin, Jinzhong Min, Shichang Kang, Guoyu Ren, Xianhong Meng. Comparison of NCEP/NCAR and ERA-40 total cloud cover with surface observations over the Tibetan Plateau. *International Journal of Climatology*. 2014, vol. 34, iss. 8, pp. 2529–2537. DOI: [10.1002/joc.3852](https://doi.org/10.1002/joc.3852).

Shikhovtsev A.Yu., Kovadlo P.G., Kiselev A.V. Astroclimatic statistics at the Sayan Solar Observatory. *Solar-Terrestrial Physics*. 2020, vol. 6, iss. 1, pp. 102–107. DOI: [10.12737/stp-61202012](https://doi.org/10.12737/stp-61202012).

Stowe L., Davis P., McClain E. Scientific basis and initial evaluation of the CLAVR-1 global clear/cloud classification algorithm for the advanced very high resolution radiometer. *J. Atmos. Ocean. Technol.* 1999, vol. 16, pp. 656–681. DOI: [10.1175/1520-0426\(1999\)016<0656:SBAIEO>2.0.CO;2](https://doi.org/10.1175/1520-0426(1999)016<0656:SBAIEO>2.0.CO;2).

Tiedtke M. A comprehensive mass flux scheme for cumulus parameterization in large-scale models. *Monthly Weather Review*. 1989, vol. 117, iss. 8, pp. 1779–1800. DOI: [10.1175/1520-0493\(1989\)117<1779:ACMFSF>2.0.CO;2](https://doi.org/10.1175/1520-0493(1989)117<1779:ACMFSF>2.0.CO;2).

Tiedtke M. Representation of clouds in large-scale models. *Monthly Weather Review*. 1993, vol. 121, iss. 11, pp. 3040–3061. DOI: [10.1175/1520-0493\(1993\)121<3040:ROCILS>2.0.CO;2](https://doi.org/10.1175/1520-0493(1993)121<3040:ROCILS>2.0.CO;2).

Zagainova Yu.S., Karavayev Yu.S. Estimation of the state of cloudiness on an 8-point scale using the histogram method from images in the visible range obtained from the full sky camera. *Solar-Terrestrial Physics (Solnechno-Zemnaya Fizika)*. 2013, vol. 23, pp. 120–128. (In Russian).

Zdor S.E., Kolin'ko V.I. *Night cloud sensor*. Patent RU 2436133 C2. 2011.

URL: <https://www.ecmwf.int> (accessed May 30, 2022).

URL: <https://www.scanex.ru> (accessed May 30, 2022).

URL: <http://ckp-rf.ru/ckp/3056> (accessed May 30, 2022).

Original Russian version: Podlesnyi S.V., Devyatova E.V., Saunkin A.V., Vasilyev R.V., published in *Solnechno-zemnaya fizika*. 2022. Vol. 8. Iss. 4. P. 102–109. DOI: [10.12737/szf-84202210](https://doi.org/10.12737/szf-84202210). © 2022 INFRA-M Academic Publishing House (Nauchno-Izdatelskii Tsentr INFRA-M)

How to cite this article

Podlesnyi S.V., Devyatova E.V., Saunkin A.V., Vasilyev R.V. Comparing methods to estimate cloud cover over the Baikal Natural Territory in December 2020. *Solar-Terrestrial Physics*. 2022. Vol. 8. Iss. 4. P. 95–102. DOI: [10.12737/stp-84202210](https://doi.org/10.12737/stp-84202210).